Mixture Models for Single-Cell Assays with Applications to Vaccine Studies

GREG FINAK[1], ANDREW MCDAVID[1], PRATIP CHATTOPADHYAY[3], MARIA

DOMINGUEZ[3], STEVE DE ROSA[1,2], MARIO ROEDERER[3], RAPHAEL GOTTARDO[1*]

[1] *Vaccine and Infectious Disease Division, Fred Hutchinson Cancer Research Center (FHCRC), Seattle, WA*

[2] *HIV Vaccine Trials Network, Fred Hutchinson Cancer Research Center (FHCRC), Seattle, WA*

[3] *Vaccine Research Center, NIAID, NIH, 40 Convent Drive, Rm 5509, Bethesda, MD 20892*

rgottard@fhcrc.org

Summary

Blood and tissue are composed of many functionally distinct cell subsets. In immunological studies, these can only be measured accurately using single-cell assays. The characterization of these small cell subsets is crucial to decipher system level biological changes. For this reason, an increasing number of studies rely on assays that provide single-cell measurements of multiple genes and proteins from bulk cell samples. A common problem in the analysis of such data is to identify biomarkers (or combinations of biomarkers) that are differentially expressed between two biological conditions (*e.g.*, before/after stimulation), where expression is defined as the proportion of cells expressing that biomarker (or biomarker combination) in the cell subset(s) of interest. Here, we present a Bayesian hierarchical framework based on a beta-binomial mixture model for testing for differential biomarker expression using single-cell assays. Our model allows the inference to be subject specific, as is typically required when assessing vaccine responses, while borrowing

*To whom correspondence should be addressed.

strength across subjects through common prior distributions. We propose two approaches for parameter estimation: an empirical-Bayes approach using an Expectation–Maximization algorithm and a fully Bayesian one based on a Markov chain Monte Carlo algorithm. We compare our method against classical approaches for single-cell assays including Fisher's exact test, a likelihood ratio test, and basic log-fold changes. Using several experimental assays measuring proteins or genes at the single-cell level and simulations, we show that our method has higher sensitivity and specificity than alternative methods. Additional simulations show that our framework is also robust to model misspecification. Finally, we demonstrate how our approach can be extended to testing multivariate differential expression across multiple biomarker combinations using a Dirichlet-multinomial model and illustrate this approach using single-cell gene expression data and simulations.

Key words: Expectation–Maximization, Markov Chain Monte Carlo, Marginal Likelihood, Bayesian Modeling, Hierarchical Modeling, Immunology, Flow Cytometry, Single-Cell Gene Expression, MIMOSA

1. INTRODUCTION

Cell populations, particularly in the immune system, are never truly homogeneous. Individual cells may be in different biochemical states that define functional but measurable differences between them. This single-cell heterogeneity is informative, but lost in assays that measure cell mixtures (*e.g.,* bulk gene expression). For this reason, single-cell assays (*e.g.,* flow, mass cytometry, single-cell gene expression) are an important tool in immunology, providing a functional snapshot of the immune system at a given time. These assays typically measure multiple biomarkers (*e.g.,* DNA content, RNA or protein expression levels, or protein phosphorylation) simultaneously on individual cells in a heterogeneous mixture such as whole blood or peripheral blood mononuclear cells (PBMC), and are used for immune monitoring of disease, vaccine research, and diagnosis of hematological malignancies (Altman *and others*, 1996; Betts *and others*, 2006; Inokuma *and others*, 2007). McDavid *and others* (2012) review the special considerations for analyzing single cell assay data. In general, special treatment of single-cell level data is warranted in order to preserve information about cell population heterogeneity.

Typically, cell-level measurements are thresholded as positive or negative so that subsets with different multivariate $+/-$ biomarkers can be obtained as Boolean combinations. For some assays (*e.g.,* flow cytometry), the positivity thresholds are set based on prior biological knowledge while for others, thresholds are given by the assay technology. This is the case for the Fluidigm's qPCR-based single-cell gene expression technology, where genes are recorded as expressed or not, at the single-cell level (McDavid *and others*, 2012). After thresholding, we obtain a Boolean matrix of N cells $\times$ K biomarkers and we can form 2^K putative cell subsets. When K is large there is a combinatorial explosion of the number of subsets, and many of these might be small or even empty. A common statistical problem is to identify subjects for whom the proportion of cells expressing a specific combination is significantly different between two experimental conditions (*e.g.,* before and after stimulation).

A motivating example from vaccine research is the need to assess the immunogenicity of a vaccine. Upon vaccination, antigen in the vaccine is taken up and presented to CD4 or CD8 T-cells via antigen presenting cells. T-cells that recognize the antigen become *activated*, produce cytokines that potentiate the immune response, and proliferate and persist in the immune system providing *memory* that can more rapidly recognize the same antigen in the future (McKinstry *and others*, 2010). This vaccine memory can be interrogated through the intracellular cytokine staining (ICS) assay, by measuring antigen-specific cytokine production in response to stimulation (Horton *and others*, 2007; De Rosa *and others*, 2004; Betts *and others*, 2006). The antigen-specific subpopulations constitute a small fraction of the total number of CD4 and CD8 T-cells (as low as 0.01%–0.1%), and a large number of cells must be collected (on the order of 50,000 to 100,000 T-cells) to ensure that changes in these cell populations can be reliably detected. Then, each individual cell is classified as either positive or negative for each cytokine based on fixed thresholds, and the number of cells matching each phenotype is counted.

Cell counts are compared between antigen stimulated and unstimulated samples from a subject to identify significant differences. *Responders* are subjects whose T-cells respond to stimulation, and the response is vaccine-specific if it exists at the post-vaccine time point but not the pre-vaccine time point. These comparisons are typically performed within a time point in order to avoid confounding vaccine effects time and because baseline samples are not always available.

Although there is no standard approach to analyzing ICS assays, current methods range from ad-hoc rules based on log-fold changes (Trigona *and others*, 2003), to non-parametric methods (Sinclair *and others*, 2004), to exact tests of 2x2 contingency tables (*e.g.*, Fisher's exact test and χ^2 test) (Horton *and others*, 2007; Proschan and Nason, 2009; Peiperl *and others*, 2010; Nason, 2006). All of these methods test subjects separately, and no information is shared across observations even though one could expect some similarities across responders (or non-responders).

The framework developed in this paper, named MIMOSA (Mixture Models for Single Cell Assays), addresses these issues. In our model, cell counts are modeled by a binomial (or multinomial in the multivariate case) distribution and information is shared across subjects through a prior distribution on the unknown proportion(s) of the binomial (or multinomial) likelihood. In order to discriminate between responders and non-responders, the prior is written as a mixture of two beta (or Dirichlet) distributions where the hyper-parameters for each mixture component are shared across subjects. This sharing of information helps regularize proportion estimates when the cell counts are small, which is typical with the single-cell assays considered here, and increases sensitivity and specificity when detecting responders. Note that we use the term 'subject' throughout the paper, but the approaches described are general and can be applied to other experimental units. Because our framework is multivariate in nature, multiple cell subsets can be modeled simultaneously, which could help detect small biological changes that are spread out across multiple cell subsets (Nason, 2006). Our paper is organized as follows; Section 2 introduces the data and notations used in the paper. In Section 3, we present our model for testing differential biomarker expression in the univariate case. Section 4 compares our approach to alternative methods and tests the robustness of our model. In Section 5, we present a multivariate extension that can be used to test multivariate biomarker differential expression and present results using single-cell gene expression data. Finally, in Section 6 we discuss our findings and future work.

2. NOTATION AND DATA

We use the following notation to describe our model. We assume that we observe cell counts from I subjects in two conditions: stimulated and unstimulated. Each cell can either be positive or negative for a biomarker. Given a set of K biomarkers, the measured cells can be classified into 2^K Boolean combinations. We denote by $n_{ik}^{(s)}$ and $n_{ik}^{(u)}$, $i = 1, \ldots, I, k = 1, \ldots, 2^K$, the observed counts for the 2^K combinations in the stimulated and unstimulated samples, respectively. We

denote by $N_i^{(s)} = \sum_k n_{ik}^{(s)}$ and $N_i^{(u)} = \sum_k n_{ik}^{(u)}$ the total number of cells measured for subject i in each sample. For ease of notation, we denote by $\mathbf{y}_i$ the vector of observed counts for subject i, i.e., $\mathbf{y}_i = (\mathbf{n}_i^{(s)}, \mathbf{n}_i^{(u)})$ where $\mathbf{n}_i^{(\cdot)} = \{n_{ik}^{(\cdot)} : k = 1, \ldots, 2^K\}$, and finally $\mathbf{y} = (\mathbf{y}_1, \ldots, \mathbf{y}_I)$.

We consider two types of immunological single-cell assays.

Flow cytometry: Our primary dataset is ICS data generated as part of a trial testing the GeoVax DNA and MVA (Modified Vaccinia Ankara) HIV vaccine in a prime–boost regimen (Goepfert *and others*, 2011). The study goal was to assess the immunogenicity of different prime–boost regimens. Here, we analyze a subset of the data consisting of 98 vaccine and placebo recipients at days 0 (pre-vaccine) and 182 (two weeks post-vaccine), focusing on CD4+ T-cell response to stimulation with HIV Envelope peptide. Three cytokines (IFN-γ, TNFα and IL2) were measured for each subject and time point, each with and without antigen stimulation. No response is expected at day 0, while day 182 is close to the immunogenicity peak and many vaccinees are expected to respond for at least some cytokines. A median of 51K and 58K T-cells were collected for the stimulated and unstimulated samples, respectively (IQR $\approx$ 37K and 43K, respectively). The empirical differences in the proportions of stimulated and unstimulated cells were on the order of 10^{-4}, with the number of positive cells typically ranging from 1–70, depending on cytokine subset.

Fluidigm single-cell gene expression: Tetramer-sorted CD8+ T-cells from sixteen subjects. T-cells isolated by flow cytometry from sixteen subjects were stimulated in blocks of four subjects with four different antigens (HIV Gag, HIV Nef, CMV pp65 tm10, and CMV pp65 nlv5) and gene expression post-stimulation was measured at the single-cell level using the BioMark system (Fluidigm) 96×96 well arrays. The expression from stimulated samples was compared to paired, unstimulated controls. In this data set, we have approximately 90 single cells per subject per stimulation condition with 96 gene expression measurements per cell.

3. Differential expression with one biomarker

Datasets like those presented here are usually analyzed in a univariate fashion to avoid being underpowered due to the large number of combinations and the potential for very small cell counts in many combinations. By univariate, we mean that we have only one positive cell subset. This cell subset can be defined by considering the expression of one biomarker alone (marginalizing over all other measured biomarkers) such as A+ (*vs.* A−), or considering a specific positive biomarker combination (and marginalizing over everything else) such as A+ or B+ (*vs.* A−/B−). Without loss of generality, we treat the univariate case as a one biomarker case (*i.e.*, $K = 1$). In this case, for a given subject, the data can be summarized in a contingency table of $+/-$ cell counts across the unstimulated and stimulated samples (Table 1).

For a given subject and stimulation, we consider a biomarker to be differentially expressed if the proportion of positive cells in the stimulated samples is different from the proportion of positive cells in the unstimulated sample. Subjects that show differential expression will be called responders for that biomarker. In this section, we are concerned with identifying differential expression one biomarker at a time, using a beta-binomial mixture model.

3.1 *Beta-binomial model*

For a given subject i, the positive cell counts for the stimulated and unstimulated samples are jointly modeled as $(n_{si}|p_{si}) \sim \text{Bin}(N_i^{(s)}, p_i^{(s)})$ and $(n_i^{(u)}|p_i^{(u)}) \sim \text{Bin}(N_i^{(u)}, p_i^{(u)})$ where $p_i^{(s)}, p_i^{(u)}$ are the unknown proportions for the stimulated and unstimulated paired samples, respectively. In order to detect responding subjects, we consider two competing models, $\mathcal{M}_0 : p_i^{(u)} = p_i^{(s)}$ and $\mathcal{M}_1 : p_i^{(u)} \neq p_i^{(s)}$. Under the null model, $\mathcal{M}_0$, there is no difference between the stimulated and unstimulated samples, and the proportions are equal (yet the cell counts can differ). Under the alternative model, $\mathcal{M}_1$, there is a difference in proportions between the two samples and the subject i is a responder. In some studies, such as the ICS data used here, the proportion of

positive cells is expected to only increase after stimulation, in which case the alternative model should be defined as $p^{(s)} > p^{(u)}$. This alternative parametrization is described in Appendix A of the Supplementary Material, and we refer to it as the one-sided model.

3.2 *Priors*

Our model shares information across all subjects using exchangeable Beta priors on the unknown proportions. For non-responders, $(p_i^{(u)}|z_i = 0) \sim \text{Beta}(\alpha^{(u)}, \beta^{(u)})$, and for responders $(p_i^{(u)}|z_i = 1) \sim \text{Beta}(\alpha^{(u)}, \beta^{(u)})$ and $(p_i^{(s)}|z_i = 1) \sim \text{Beta}(\alpha^{(s)}, \beta^{(s)})$, where z_i is an indicator variable equal to one if subject i is a responder, *i.e.*, $\mathcal{M}_1$ is true, and zero otherwise, and $\alpha^{(u)}, \beta^{(u)}, \alpha^{(s)}, \beta^{(s)}$ are unknown hyper-parameters shared across all subjects. Note that the parameters $\alpha^{(u)}$ and $\beta^{(u)}$ are shared across both models, whereas $\alpha^{(s)}$ and $\beta^{(s)}$ are only present in the alternative model. Finally, we assume that $z_i \sim \text{Be}(w)$ are independent draws from a Bernoulli distribution with probability w, where w represents the (unknown) proportion of responders. It follows that marginally, *i.e.*, after integrating z_i, the $p_i^{(u)}$ and $p_i^{(s)}$ are then jointly distributed as a mixture of a one dimensional Beta distribution and a product of two Beta distributions (with a possible constraint), with mixing parameter w. Treating the z_i's as missing data, the unknown parameter vector $\boldsymbol{\theta} \equiv (\alpha^{(u)}, \beta^{(u)}, \alpha^{(s)}, \beta^{(s)}, w)$ can be estimated in an Empirical-Bayes fashion using an Expectation-Maximization algorithm (Dempster *and others*, 1977) as described in Section 3.3. We also describe a fully Bayesian model where the hyperparameters $\alpha^{(u)}, \beta^{(u)}$, $\alpha^{(s)}$, and $\beta^{(s)}$ are each given vague exponential priors with mean 10^3, and w is assumed to be drawn from a uniform distribution between 0 and 1. In this case, all parameters will be estimated via a Markov chain Monte Carlo algorithm as described in Section 3.3.

3.3   *Parameter estimation*

In our proposed EM and MCMC algorithms, we greatly simplify our calculations by directly utilizing the marginal likelihoods, L_0 and L_1, obtained after marginalizing $p_i^{(s)}$ and $p_i^{(u)}$ from the null and alternative likelihoods. Given the conjugacy of the priors, the marginal likelihoods L_0 and L_1 are available in closed-forms (Appendix B, Supplementary Material).

Assuming that the missing data, $z_i, i = 1, \ldots, I$, are known, we define the complete data log-likelihood:

$$l(\boldsymbol{\theta}|\mathbf{y}, \mathbf{z}) = \sum_i z_i l_0(\alpha^{(u)}, \beta^{(u)}|\mathbf{y}_i) + (1 - z_i)l_1(\alpha^{(u)}, \beta^{(u)}, \alpha^{(s)}, \beta^{(s)}|\mathbf{y}_i) + z_i \log(w) + (1 - z_i)\log(1 - w),$$

$$(3.1)$$

where l_0 and l_1 are the log marginal-likelihoods and $\boldsymbol{\theta} \equiv (\alpha^{(u)}, \beta^{(u)}, \alpha^{(s)}, \beta^{(s)}, w)$ is the vector of parameters to be estimated. In the one-sided case, the alternative prior specification must satisfy the constraint $p^{(s)} > p^{(u)}$, and the marginal likelihood derivation involves the calculation of a normalizing constant that is not available in closed-form but can easily be estimated. All calculations for the one-sided case are described in Appendix A of the Supplementary Material.

EM algorithm: Given an estimate of the model parameter vector $\tilde{\boldsymbol{\theta}} = \left\{ \tilde{\alpha}^{(u)}, \tilde{\beta}^{(u)}, \tilde{\alpha}^{(s)}, \tilde{\beta}^{(s)}, \tilde{w} \right\}$ and the data $\mathbf{y}$, the E step consists of calculating the posterior probabilities of differential expression, defined by $\tilde{z}_i \equiv \Pr(z_i = 1|\mathbf{y}, \tilde{\boldsymbol{\theta}})$:

$$\Pr(z_i = 1|\mathbf{y}, \tilde{\boldsymbol{\theta}}) = \frac{\tilde{w} \cdot \mathrm{L}_1(\tilde{\alpha}^{(u)}, \tilde{\beta}^{(u)}, \tilde{\alpha}^{(s)}, \tilde{\beta}^{(s)}, |\mathbf{y}_i)}{(1 - \tilde{w}) \cdot \mathrm{L}_0(\tilde{\alpha}^{(u)}, \tilde{\beta}^{(u)}|\mathbf{y}_i) + \tilde{w} \cdot \mathrm{L}_1(\tilde{\alpha}^{(u)}, \tilde{\beta}^{(u)}, \tilde{\alpha}^{(s)}, \tilde{\beta}^{(s)}|\mathbf{y}_i)}.$$

The M-step then consist of optimizing the complete-data log-likelihood over $\boldsymbol{\theta}$ after replacing z_i by $\tilde{z}_i$ in (3.1). Straightforward calculations lead to $\tilde{w} = \sum_i \tilde{z}_i/I$, but unfortunately no closed form solutions exist for the remaining parameters. We use numerical optimization as implemented in R's *optim* function to estimate the remaining parameters (Ihaka and Gentleman, 1996). We initialize the z_i's using Fisher's exact test to assign each observation to either the null or alternative components and then use the estimated z_i's to estimate the $p_i^{(u)}$'s and $p_i^{(s)}$'s and use these to set the hyper-parameters to their method-of-moments estimates.

MCMC algorithm: We generated realizations from the posterior distribution via MCMC algorithms (Gelfand and Smith, 1990). All updates were done via Metropolis-Hastings sampling except for the z_i's and w that were performed via Gibbs sampling. Details about the algorithms and implementation are given in Appendix B of the Supplementary Material.

4. RESULTS

We evaluated and compared the performance of MIMOSA against Fisher's exact test, a likelihood ratio test, and log fold-change by ROC (receiver operator characteristic) curve analysis and by compared the *observed FDR* (false discovery rate) against the *nominal FDR* (expected false discovery rate) for the ICS data. A false discovery is defined as a day 0 sample or a sample from a placebo recipient (expected non-responders) that is identified as a responder by an algorithm. For MIMOSA, the FDR was computed using the approach of Newton *and others* (2004) whereas for all other methods FDR control was done using the approach of Benjamini and Hochberg (1995).

4.1 *ICS*

In the ICS data we considered observations from vaccinees at day 0 or from placebos at day 0 or 182 as *true negatives* in that we do not expect to observe a response in those samples. Observations from vaccinees at day 182 were considered *true positives* in that a response is expected assuming a 100% response rate. This assumption was required, since we do not have independent, external measurement of the true response. Under these assumptions, the MIMOSA model has higher sensitivity and specificity than method compared here for discriminating vaccine responders and non-responders as shown by the ROC curves on Figure 1, panels A,C,E. At an FDR between 10-20%, MIMOSA would lead to about 20% more true positives being detected. In addition, MIMOSA gave estimates of the observed false discovery rate that are better or comparable to competing methods (Figure 1, panels B,D,F). Here we present the results based

on IL2 and IFN-γ alone as well as the subset expressing IL2 or IFN-γ that were used in the original study (Goepfert *and others*, 2011). These results are consistent for other cytokines and cytokine combinations, including higher order combinations (Supplementary Figure 1). We also evaluated, through simulation, what would happen to the ROC curves when our assumption of 100% response rate was false (*i.e.*, when not all day 182 vaccinees are responders, Supplementary Figure 2), and found that we are potentially underestimating the sensitivity of all methods considered here due to non-responders at day 182. Nonetheless, the ranking of the methods remained consistent and the conclusions from the ROC analysis still hold.

We verified the assumption of a common distribution for the $p_i^{(u)}$ across subjects by examining the empirical estimates of $p_i^{(u)}$ and the density of the Beta distribution with parameters $\hat{\alpha}^{(u)}, \hat{\beta}^{(u)}$ fitted to ENV-1-PTEG stimulated CD4+/IFN–γ+ T–cell ICS data (Supplementary Figure 3). The effect of information sharing on the sensitivity and specificity of the model was also investigated by varying the number of subjects in simulations (Supplementary Figure 4). Our model performed well when as few as 20 subjects were included, although the nominal false discovery rate overestimated observed false discovery rate.

4.2   *Single-cell gene expression*

We applied the MIMOSA model to the Fluidigm single-cell gene expression data set. We used the two-sided MIMOSA model because genes could be regulated upward or downward upon stimulation. In order to detect stimulation specific changes of expression, we fit our model separately to each gene within each stimulation. The results show that MIMOSA identifies stimulation-specific differences in the proportions of cells expressing each gene while preserving inter-subject variability (Figure 2 A). These patterns evident in the posterior probabilities (Figure 2 A) closely match the empirical estimates of the differences in proportions (Figure 2 B). As a comparison, we also fit the model combining information across all stimulations (Figure 2 C). Although this leads to a

sensible clustering by stimulation, the observed pattern does not agree as well with the empirical differences. A similar analysis applying a two-sided Fisher's exact test to each sample and gene, and clustering the signed FDR adjust q-values (Figure 2 D) does not reveal stimulation-specific patterns, with the exception of CMV pp65 nlv5 stimulation. At an FDR of 10%, Fisher's exact test identified 13 significant genes, while MIMOSA identified 46 significant genes. The 13 genes identified by Fisher's method were a subset of those identified by MIMOSA. These results suggest that fitting a stimulation–specific model is the right approach since information is shared across subjects that are expected to exhibit similar behavior.

4.3 *Simulation Studies*

We examined the performance of the constrained ($p^{(s)} > p^{(u)}$) and unconstrained ($p^{(s)} \neq p^{(u)}$) beta-binomial mixture models via simulations. For the simulation, we used hyper–parameters estimated from a one-sided MIMOSA model fit to ICS data (univariate IL2+) from the primary immunogenicity time point. We simulated data from this constrained model with 200 subjects, a response rate of 50%, $N = 10,000$, 25,000, and 50,000 cells, and ten independent realizations of data for each N. We fit the one-sided MIMOSA model to this data and evaluated the sensitivity and specificity to identify responders and non-responders through ROC analysis. MIMOSA was compared against the same methods as in section 4.1. We repeated this procedure for the two-sided models fit to two-sided data, and compared the ability of each method to properly control the FDR. For both the constrained and unconstrained simulations, MIMOSA exhibited superior sensitivity and specificity than competing methods, even with fewer subjects and smaller cell counts (Figure 3 A,C, and Supplementary Figures 4 A and 5 A). MIMOSA also provided better control of the FDR than competing approaches (Figure 3, panels B, D, Supplementary Figures 4 B and 5 B).

To assess the sensitivity of the model to deviations from model assumptions, we simulated data

with the cell proportions drawn from truncated normal distributions with support $(0, 1)$, rather than beta distributions. The means and variances of the truncated normal distributions were set to the MLE of the beta distributions defined by the hyper–parameters α and β estimated from the ICS data set (Supplementary Figure 5 C,D). Even under these departures from the model assumptions, the unconstrained MIMOSA model outperformed competing methods.

5. Differential expression across biomarker combinations

Our beta-binomial model described in Section 3.1 can be generalized to a Dirichlet-multinomial model to assess differential expression across multiple biomarker combinations. As described in the data section, we now have counts for each biomarker combination, denoted by $\mathbf{n}_i^{(s)} = \{n_{ik}^{(s)} : k = 1, \ldots, 2^K\}$ and $\mathbf{n}_i^{(u)} = \{n_{ik}^{(u)} : k = 1, \ldots, 2^K\}$.

In our multivariate model, the beta distribution is replaced by a multinomial distribution. Thus the observed data are drawn from $(\mathbf{n}_i^{(u)}|\mathbf{p}_i^{(u)},) \sim \mathcal{M}(N_i^{(u)}, \mathbf{p}_i^{(u)})$ and $(\mathbf{n}_i^{(s)}|\mathbf{p}_i^{(s)}) \sim \mathcal{M}(N_i^{(s)}, \mathbf{p}_i^{(s)})$, where $N_i^{\{s,u\}} = \sum_{k=1}^{2^K} n_{ik}^{\{s,u\}}$ are the number of cells collected and $\mathbf{p}_i^{(u)}$ and $\mathbf{p}_i^{(s)}$ are the unknown proportions for the unstimulated and stimulated samples, respectively.

As in the one-biomarker case, we share information across subjects using an exchangeable prior on the unknown proportions. The beta priors in 3.2 are replaced by Dirichlet distributions. The indicator variable z_i is defined as in Section 3.2. As in the beta-binomial case, both EM and MCMC algorithms can be used for parameter estimation. When using a fully Bayesian approach via MCMC, we use the same priors for $\boldsymbol{\alpha}^{\{u,s\}}$ and w as for the beta-binomial model.

We again make use of the marginal likelihoods available in closed form (see Appendix C of the Supplementary Material). The estimation procedures (both EM and MCMC) for the Dirichlet–multinomial are the same as for the beta-binomial model except that the number of parameters to estimate is larger. We initialize the z_i in the EM algorithm with the positivity calls from the multivariate Fisher's exact test. In our experience, the performance of the EM algorithm greatly

deteriorates for $K > 3$, and is more dependent on the initial values and can fail to converge in many instances. Although our MCMC algorithm is slightly more computational, it does not suffer from this problem and provides a robust alternative when K is large. More details are given in Appendix C of the Supplementary Material.

5.1   *Polyfunctionality in Fluidigm Single-Cell Gene Expression Data*

As a proof-of-concept, we applied our multivariate MIMOSA model to two specific genes in the Fluidigm data, namely CCR7 and GZMK. For this example $K = 2$ and we have four possible subsets. In Figure 4 we show heatmaps of the $\log_2$ counts of cells expressing all combinations of the CCR7 and GZMK genes in unstimulated and stimulated samples, as well as for the log_2 of the sum of the counts of the 3 positive subsets. The number of CCR7-GZML+ cells increases upon stimulation, while the number of CCR7+GZMK- cells decreases. The typical approach to analyzing poly-functional populations from intracellular cytokine staining data by summing the counts over all polyfunctional cell populations (*i.e.*, cells expressing CCF7+ or GZMK+), would not be appropriate in this case, since changes in the counts are bidirectional and their sum is near zero. The multivariate MIMOSA model tests for any difference across all polyfunctional cell subsets and detects significant differences in 12 of the 16 subjects (Figure 4 A, dark labels), whereas the standard approach detects no differences (Figure 4 B). Testing all combinations simultaneously is also an advantage over performing multiple univariate tests on the subject combinations, which requires multiplicity adjustment and a potential loss of power.

Since the Fluidigm data set has a limited number of observations (100 cells and 16 samples), we could not look at more than two biomarkers at once. Therefore, we performed simulations in eight dimensions to assess the performance of the multivariate MIMOSA model on the resulting 2x8 tables (Supplementary Figure 6 A,B). These results show that multivariate MIMOSA outperformed competing methods even when cell counts were small and at small effect sizes. MIMOSA

also provided better FDR control than competing approaches (Supplementary Figure 6 B).

6. Discussion

The development of effective statistical methods to detect differences in gene or protein expression at the single-cell level is becoming increasingly important as single-cell assays become more routine and sequencing at the single-cell level eventually becomes practical (Ramsköld *and others*, 2012). Current approaches, such as the t-test, χ^2 test and Fisher's exact test are for the most part simplistic, and resulting inference can be quite sub-optimal, especially when the cell counts are small. Most importantly, these methods do not share information across samples, resulting in less power to detect true differences than empirical-Bayes and hierarchical modeling approaches, which are widely applied in the microarray literature (Newton *and others*, 2004; Gottardo *and others*, 2006; Lo and Gottardo, 2007). In addition, most of these methods are univariate in nature and inappropriate for high-dimensional, next-generation single-cell assays.

The MIMOSA model uses a mixture framework to model counts in experimental subjects across multiple conditions. Information is shared across subjects through exchangeable priors, increasing the power to detect true differences compared to competing methods, even when the underlying model assumptions are violated (Figures 3 and Supplementary Figure 5 B). Although in some instances the FDR was not well controlled by any method tested (Supplementary Figure 1A), volcano plots of effect size vs posterior probability of response show these false positives are pre–vaccine subjects exhibiting response to stimulation (Supplementary Figure 7). Such variability is occasionally expected due to assay failures or biological variation.

MIMOSA is fit to dichotomized data (cells are positive or negative). While this is the standard approach for ICS data analysis, it is believed that the magnitude (fluorescence intensity) of the signal also carries information. For single-cell gene expression data, most methods have focused on differences in the continuous part of the signal while using the discrete on/off nature for

pre-filtering (Flatz *and others*, 2011). The ability of MIMOSA to identify stimulation-specific expression patterns in the Fluidigm data demonstrates not only the broader utility of the method, but demonstrates that biologically relevant signal is present in the frequency of gene expression (Figure 2). We have shown elsewhere that changes in both the frequency of expression and expression level are informative (McDavid *and others*, 2012), and extensions of the model that incorporate the continuous component are warranted in the future. Although we used two single-cell assay platforms as motivating examples, our MIMOSA model can be applied to any type of single-cell assay where cells are dichotomized into positive and negative subsets.

Detecting differences in poly-functional cell populations is important in immunology, since it allows the identification of more homogeneous cell populations (Milush *and others*, 2009). In the context of HIV, poly-functional cell populations have been shown to be correlated with long-term disease non-progression, while in the context of vaccination studies poly–functional responses have been correlated with protection from disease (Betts *and others*, 2006; Darrah *and others*, 2007; Precopio *and others*, 2007, e.g.). In the ICS data used here, the stimulation is expected to only increase the number of antigen specific cells. The univariate MIMOSA model allows us to constrain the alternative hypothesis to the case $p^{(s)} > p^{(u)}$, where the proportion of cells in the stimulated sample is strictly greater than the proportion of cells in the unstimulated sample, and is ideal for this situation. Hence, if a specific cell subset expressing multiple biomarkers is differentially expressed, then differential expression based on the marginal cell counts should also be detectable. As such, identifying poly-functional cytokine profiles from ICS data could be done in an iterative way. First, univariate tests on marginal populations are performed, then specific cell subsets expressing the positive biomarkers detected are tested. However, this iterative (univariate) approach might not be satisfactory due to the large number of combinations that need to be tested. A multivariate approach might be preferable. In that case, as others have pointed out, in order to have the most power to detect a true difference, the statistical test

should only take into account the cytokine combinations of interest (Nason, 2006).

When changes are two-sided (as with Fluidigm), differences in poly-functional cell populations are not always detectable since differences may cancel in the marginal populations (Figure 4 B). In this case, the use of multivariate models, as our Dirichlet-multinomial model, will be important (Figure 4 A). Unfortunately, the limited number of samples in the Fluidigm data prevented us from looking at co-expression involving more than two genes. In the case of more than two biomarkers, the number of parameters for our model is $2^{K+1}+1$, which is large even for moderate values of K. Even for $K = 4$, we would need a large number of subjects and cells to properly estimate the 33 parameters. A solution would be to explore alternative model parameterizations that could be used to reduce the number of required parameters. For example, one could assume that the hyper-parameters are constant across biomarker combinations, $i.e.$, $\alpha_k^{\{s,u\}} = \alpha^{\{s,u\}}$ for all k, and the number of parameters would be reduced to 3 for any K. In reality, such a model would be unrealistic given that certain stimulations are known to induce expression of certain biomarkers more than others. More exploratory work will need to be done in this area once high dimensional single-cell level data with large number of samples become available.

All of the results presented here were obtained with an R and C++ implementation the MIMOSA models, freely available at (`http://www.github.org/RGLab/MIMOSA`).

Supplementary Materials

Appendix A, B, and C and Supplementary Figures 1–7 referenced in Sections 2–5 are available in the Supplementary Material.

Acknowledgments

References

ALTMAN, J D, MOSS, P A, GOULDER, P J, BAROUCH, D H, MCHEYZER-WILLIAMS, M G, BELL, J I, MCMICHAEL, A J AND DAVIS, M M. (1996, October). Phenotypic analysis of antigen-specific T lymphocytes. *Science (New York, NY)* **274**(5284), 94–96.

BENJAMINI, YOAV AND HOCHBERG, YOSEF. (1995). Controlling the false discovery rate: A practical and powerful approach to multiple testing. *Journal of the Royal Statistical Society. Series B (Methodological)* **57**(1), pp. 289–300.

BETTS, MICHAEL R, NASON, MARTHA C, WEST, SADIE M, DE ROSA, STEPHEN C, MIGUELES, STEPHEN A, ABRAHAM, JONATHAN, LEDERMAN, MICHAEL M, BENITO, JOSE M, GOEPFERT, PAUL A, CONNORS, MARK, ROEDERER, MARIO *and others*. (2006, June). Hiv nonprogressors preferentially maintain highly functional hiv-specific cd8+ t cells. *Blood* **107**(12), 4781–4789.

DARRAH, PATRICIA A, PATEL, DIPTI T, DE LUCA, PAULA M, LINDSAY, ROSS W B, DAVEY, DYLAN F, FLYNN, BARBARA J, HOFF, SØREN T, ANDERSEN, PETER, REED, STEVEN G, MORRIS, SHELDON L, ROEDERER, MARIO *and others*. (2007, July). Multifunctional TH1 cells define a correlate of vaccine-mediated protection against Leishmania major. *Nature Medicine* **13**(7), 843–850.

DE ROSA, STEPHEN C, LU, FABIEN X, YU, JOANNE, PERFETTO, STEPHEN P, FALLOON,

JUDITH, MOSER, SUSAN, EVANS, THOMAS G, KOUP, RICHARD, MILLER, CHRISTOPHER J AND ROEDERER, MARIO. (2004, November). Vaccination in humans generates broad t cell cytokine responses. *J Immunol* **173**(9), 5372–5380.

DEMPSTER, A.P., LAIRD, N.M. AND RUBIN, D.B. (1977). Maximum likelihood from incomplete data via the em algorithm. *Journal of the Royal Statistical Society. Series B (Methodological)* **39**(1), 1–38.

FLATZ, LUKAS, ROYCHOUDHURI, RAHUL, HONDA, MITSUO, FILALI-MOUHIM, ABDELALI, GOULET, JEAN-PHILIPPE, KETTAF, NADIA, LIN, MIN, ROEDERER, MARIO, HADDAD, ELIAS K, SÉKALY, RAFICK P *and others*. (2011, April). Single-cell gene-expression profiling reveals qualitatively distinct CD8 T cells elicited by different gene-based vaccines. *Proceedings of the National Academy of Sciences* **108**(14), 5724–5729.

GELFAND, ALAN E AND SMITH, ADRIAN F M. (1990, June). Sampling-Based Approaches to Calculating Marginal Densities.

GOEPFERT, P A, ELIZAGA, M L, SATO, A, QIN, L, CARDINALI, M, HAY, C M, HURAL, J, DEROSA, S C, DEFAWE, O D, TOMARAS, G D, MONTEFIORI, D C, XU, Y, LAI, L, KALAMS, S A, BADEN, L R, FREY, S E, BLATTNER, W A, WYATT, L S, MOSS, B, ROBINSON, H L *and others*. (2011, January). Phase 1 Safety and Immunogenicity Testing of DNA and Recombinant Modified Vaccinia Ankara Vaccines Expressing HIV-1 Virus-like Particles. *J Infect Dis* **203**(5), 610–619.

GOTTARDO, R, RAFTERY, A E, KA YEE, Y AND BUMGARNER, R. (2006, March). Bayesian robust inference for differential gene expression in microarrays with multiple samples. *Biometrics* **62**, 10–18.

HORTON, H, THOMAS, EP, STUCKY, JA, FRANK, I, MOODIE, Z, HUANG, Y, CHIU, YL,

MCELRATH, MJ AND DE ROSA, SC. (2007). Optimization and validation of an 8-color intra-cellular cytokine staining (ics) assay to quantify antigen-specific t cells induced by vaccination. *Journal of immunological methods* **323**(1), 39–54.

IHAKA, R AND GENTLEMAN, R. (1996). R: A language for data analysis and graphics. *Journal of Computational and Graphical Statistics* **5**(3), 299–314.

INOKUMA, MARGARET, DELA ROSA, CORAZON, SCHMITT, CHARLES, HAALAND, PERRY, SIEBERT, JANET, PETRY, DOUGLAS, TANG, MENGXIANG, SUNI, MARIA A, GHANEKAR, SMITA A, GLADDING, DAIVA, DUNNE, JOHN F, MAINO, VERNON C, DISIS, MARY L *and others.* (2007, August). Functional T cell responses to tumor antigens in breast cancer patients have a distinct phenotype and cytokine signature. *J Immunol* **179**(4), 2627–2633.

LO, KENNETH AND GOTTARDO, RAPHAEL. (2007). Flexible empirical Bayes models for differ-ential gene expression. *Bioinformatics* **23**(3), 328–335.

MCDAVID, ANDREW, FINAK, GREG, CHATTOPADYAY, PRATIP K., DOMINGUEZ, MARIA, LAM-OREAUX, LAURIE, MA, STEVEN S., ROEDERER, MARIO AND GOTTARDO, RAPHAEL. (2012, December). Data Exploration, Quality Control and Testing in Single-Cell qPCR-Based Gene Expression Experiments. *Bioinformatics* **29**(4), 9.

MCKINSTRY, K KAI, STRUTT, TARA M AND SWAIN, SUSAN L. (2010, May). The potential of CD4 T-cell memory. *Immunology* **130**(1), 1–9.

MILUSH, JEFFREY M, LONG, BRIAN R, SNYDER-CAPPIONE, JENNIFER E, CAPPIONE, AMEDEO J, YORK, VANESSA A, NDHLOVU, LISHOMWA C, LANIER, LEWIS L, MICHAËLSSON, JAKOB AND NIXON, DOUGLAS F. (2009, November). Functionally distinct subsets of human NK cells and monocyte/DC-like cells identified by coexpression of CD56, CD7, and CD4. *Blood* **114**(23), 4823–4831.

NASON, M. (2006, August). Patterns of Immune Response to a Vaccine or Virus as Measured by Intracellular Cytokine Staining in Flow Cytometry: Hypothesis Generation and Comparison of Groups. *Journal of Biopharmaceutical Statistics* **16**(4), 483–498.

NEWTON, MICHAEL A, NOUEIRY, AMINE, SARKAR, DEEPAYAN AND AHLQUIST, PAUL. (2004, April). Detecting differential gene expression with a semiparametric hierarchical mixture method. *Biostatistics (Oxford, England)* **5**(2), 155–76.

PEIPERL, LAURENCE, MORGAN, CECILIA, MOODIE, ZOE, LI, HONGLI, RUSSELL, NINA, GRA-HAM, BARNEY S, TOMARAS, GEORGIA D, DE ROSA, STEPHEN C, MCELRATH, M JULIANA AND THE NIAID HIV VACCINE TRIALS NETWORK. (2010, October). Safety and immuno-genicity of a replication-defective adenovirus type 5 hiv vaccine in ad5-seronegative persons: A randomized clinical trial (hvtn 054). *PLoS ONE* **5**(10), e13579.

PRECOPIO, MELISSA L, BETTS, MICHAEL R, PARRINO, JANIE, PRICE, DAVID A, GOSTICK, EMMA, AMBROZAK, DAVID R, ASHER, TEDI E, DOUEK, DANIEL C, HARARI, ALEXANDRE, PANTALEO, GIUSEPPE, BAILER, ROBERT, GRAHAM, BARNEY S, ROEDERER, MARIO *and others*. (2007, June). Immunization with vaccinia virus induces polyfunctional and phenotypically distinctive CD8(+) T cell responses. *The Journal of experimental medicine* **204**(6), 1405–1416.

PROSCHAN, MICHAEL A AND NASON, MARTHA. (2009, March). Conditioning in 2 x 2 tables. *Biometrics* **65**(1), 316–322.

RAMSKÖLD, DANIEL, LUO, SHUJUN, WANG, YU-CHIEH, LI, ROBIN, DENG, QIAOLIN, FARI-DANI, OMID R, DANIELS, GREGORY A, KHREBTUKOVA, IRINA, LORING, JEANNE F, LAU-RENT, LOUISE C, SCHROTH, GARY P *and others*. (2012, July). Full-length mRNA-Seq from single-cell levels of RNA and individual circulating tumor cells. *Nature Biotechnology* **30**, 777–82.

SINCLAIR, ELIZABETH, BLACK, DOUGLAS, EPLING, C LORRIE, CARVIDI, ALEXANDER, JOSE-
FOWICZ, STEVEN Z, BREDT, BARRY M AND JACOBSON, MARK A. (2004). CMV antigen-
specific CD4+ and CD8+ T cell IFNgamma expression and proliferation responses in healthy
CMV-seropositive individuals. *Viral immunology* **17**(3), 445–454.

TRIGONA, WENDY L, CLAIR, JAMES H, PERSAUD, NATASHA, PUNT, KARA, BACHINSKY,
MARGARET, SADASIVAN-NAIR, USHA, DUBEY, SHERI, TUSSEY, LYNDA, FU, TONG-MING
AND SHIVER, JOHN. (2003, July). Intracellular staining for HIV-specific IFN-gamma pro-
duction: statistical analyses establish reproducibility and criteria for distinguishing positive
responses. *Journal of interferon & cytokine research : the official journal of the International
Society for Interferon and Cytokine Research* **23**(7), 369–377.

Table 1. 2 x 2 contingency table of counts for biomarker positive and negative cells
between stimulated (s) and unstimulated (u) conditions for a given subject i.

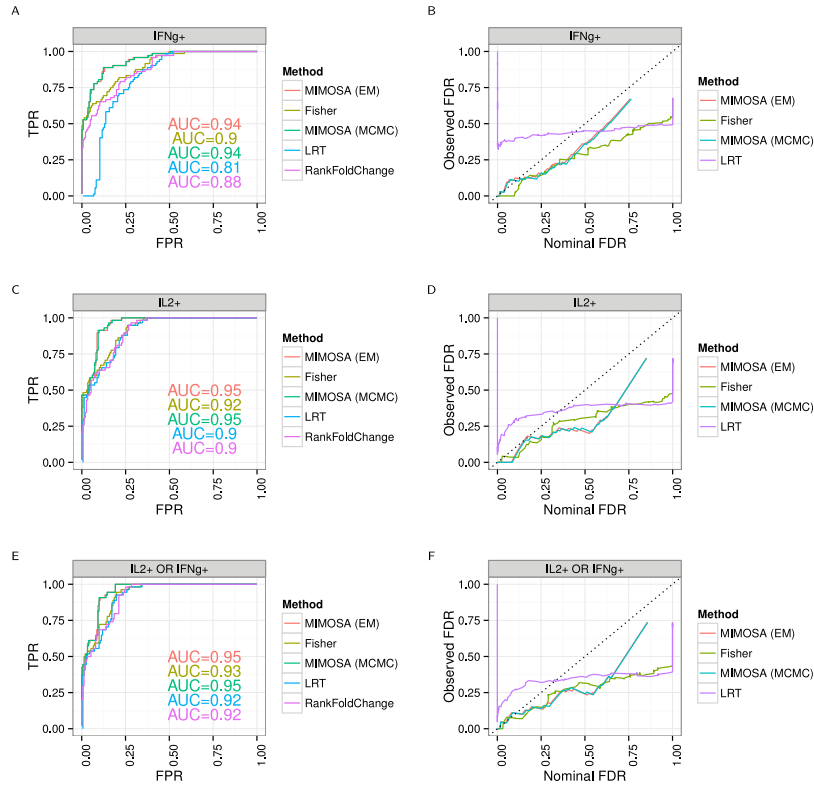|	Biomarker	
	Negative	Positive
Stimulated	$N_i^{(s)} - n_i^{(s)}$	$n_i^{(s)}$
Unstimulated	$N_i^{(u)} - n_i^{(u)}$	$n_i^{(u)}$

Fig. 1. Performance of MIMOSA (EM and MCMC implementations, one-sided model) and competing methods on ICS data from the example flow cytometry data set. Sensitivity and specificity (ROC analysis) as well as observed and nominal false discovery rates for positivity calls from CD4+ T-cells stimulated with A-B) ENV-1-PTEG and expressing IFN-γ or C-D) ENV-1-PTEG and expressing IL2. E-F) ENV-1-PTEG and expressing IFN-γ or IL2. ROC and FDR plots of other cytokine combinations can be found in Supplementary Figure 1.This figure appears in color in the electronic version of this article.
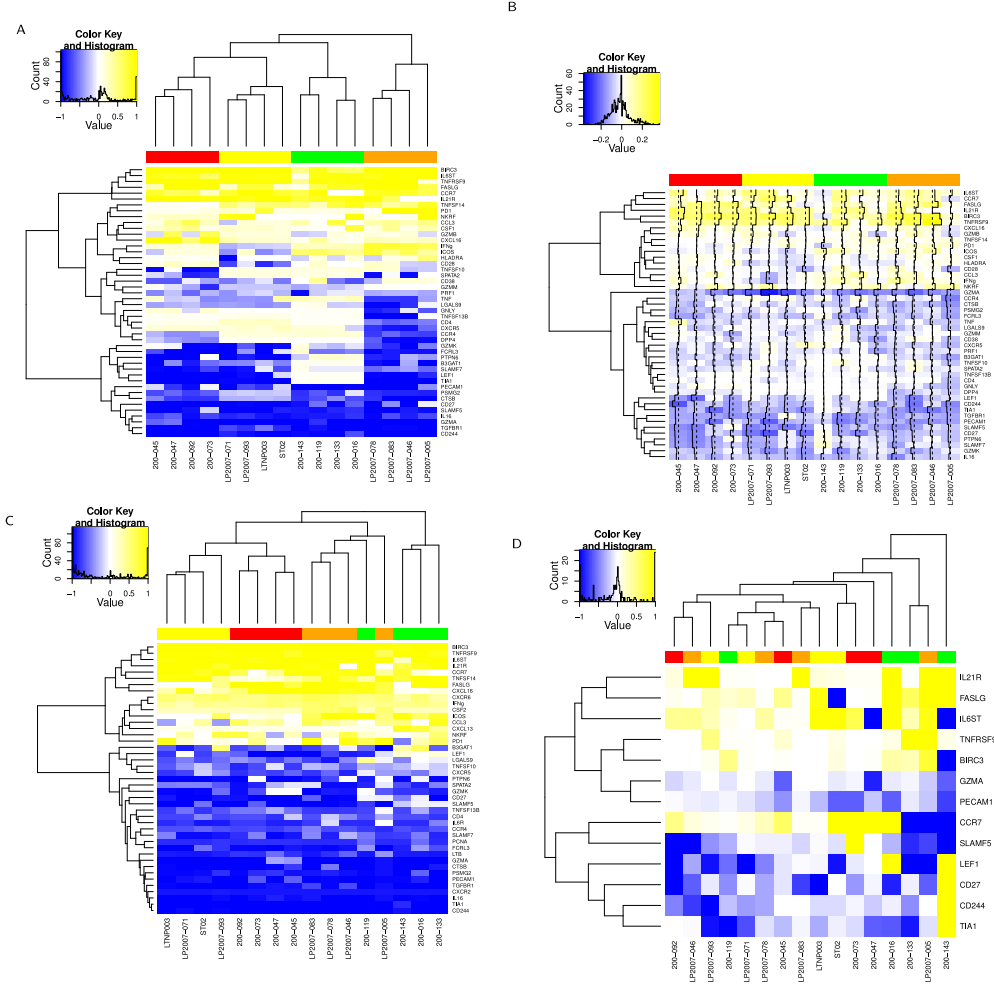
Fig. 2. Signed posterior probability and difference in empirical in proportions of single-cells expressing each gene on a 96x96 Fluidigm array. The posterior probability of response times the sign of the change in expression is shown in A) (red indicates a decrease, green an increase, relative to the control) for a model fit to each stimulation and gene separately. Columns and rows are clustered based on these signed posterior probabilities. B) The empirical differences in proportion of cells expressing a gene in the stimulated vs. control samples. Rows and columns are ordered as in A) for comparison. The traces show the deviations of each cell from zero. Colors along the columns denote different stimulations (green: CMV pp65 nlv5, red: HIV Gag, orange: HIV Nef, yellow: CMV pp65 tm10). C) Signed posterior probabilities for a model fit per gene but across all stimulations simultaneously. D) Clustering of the signed q-values from Fisher's exact test. All genes were significant at, or below, the 10% FDR level. This figure appears in color in the electronic version of this article.
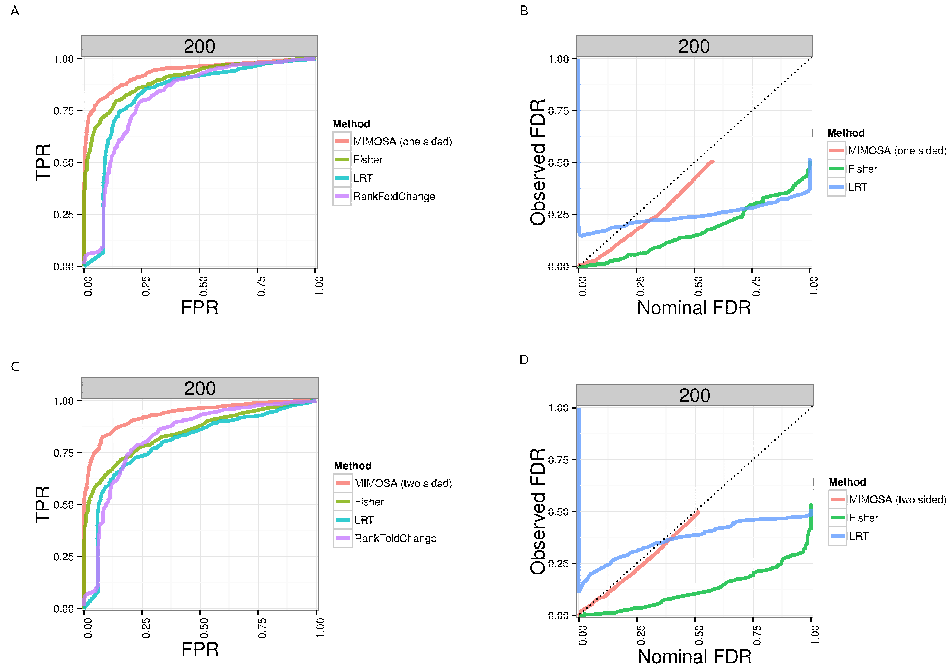
Fig. 3. Comparison of positivity detection methods on data simulated from the one-sided and two–sided models. Ten simulations were generated at an N of 50,000 total counts using hyper-parameter estimates from real ICS data (IFN-γ expressing CD4+ T-cells stimulated with ENV-1-PTEG from HVTN065) with a five-fold effect size between responder and non-responder components. A) Average ROC curve over the 10 simulated data sets (N=50,000), one–sided B) Average observed and nominal false discovery rate over 10 simulated data sets (N=50,000), one–sided. C) Average ROC curves, two–sided model. D) Average observed and nominal FDR, two–sided model. Curves are shown for MIMOSA, Fisher's exact test, the likelihood ratio test, and log fold-change. Results for MIMOSA fit to a model violating model assumptions, as well as other values of N (number of cells) and values of I (number of subjects) are in Supplementary Figures 3 and 4. This figure appears in color in the electronic version of this article.
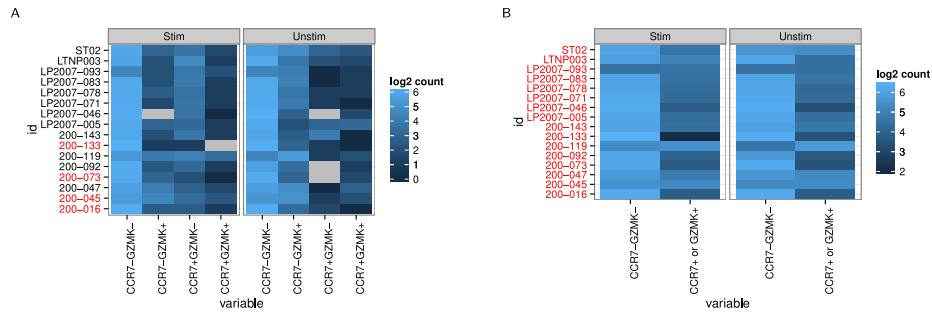

Fig. 4. Counts of cells expressing A) different combinations of CCR7 and GZMK genes in the unstimulated and stimulated conditions (+/+,+/-,-/+,-/-), and for B) the marginalized positive counts in stimulated and unstimulated conditions. No difference is observed from the marginalized counts, while multivariate MIMOSA detects a difference between stimulated and unstimulated conditions in 12 of 16 samples, while Fisher's test detects 9 of 16. Sample names highlighted in red identify those where MIMOSA did not detect a difference. This figure appears in color in the electronic version of this article.